

Exploring memory-burdened primordial black holes with ultra-high-energy cosmic-rays

Antonio Ambrosone,^{1,2,*} Marco Chianese,^{3,4,†} and Carmelo Evoli^{1,2,‡}

¹*Gran Sasso Science Institute (GSSI), Viale Francesco Crispi 7, 67100 L'Aquila, Italy*

²*INFN-Laboratori Nazionali del Gran Sasso (LNGS), via G. Acitelli 22, 67100 Assergi (AQ), Italy*

³*Scuola Superiore Meridionale, Via Mezzocannone 4, 80138 Napoli, Italy*

⁴*INFN - Sezione di Napoli, Complesso Universitario Monte Sant'Angelo, 80126 Napoli, Italy*

Quantum backreaction effects may quench Hawking evaporation through a “memory burden”, allowing primordial black holes (PBHs) with formation masses well below 10^{15} g to survive to the present and contribute to the dark matter. We show that ultra-high-energy cosmic rays (UHECRs) provide a powerful and previously unexplored probe of this scenario. We compute the proton and neutron emission from memory-burdened PBHs, including the Galactic-halo contribution and the extragalactic proton component, and confront it with the Pierre Auger Observatory proton spectrum and its EeV neutron limits from the Galactic plane. This yields new constraints on the PBH dark-matter fraction as a function of the PBH formation mass and the evaporation-suppression parameter k . For $k \gtrsim 3$ the non-observation of ultra-high-energy protons leads to bounds competitive with those from UHE gamma rays, while neutron limits remain comparable to high-energy neutrino constraints. Our results highlights the key role of multi-messenger astronomy in constraining beyond-the-standard-model scenarios.

I. INTRODUCTION

Ultra-High-Energy Cosmic Rays (UHECRs) are the most energetic particles ever observed reaching energies of the order of 10^{20} eV [1, 2]. Despite their sources remain yet to be discovered, UHECRs allow us to probe fundamental physics at energies not accessible by any other experiment on Earth [3–13]. In this article, for the first time, we explore the constraints imposed by UHECRs on memory-burdened Primordial Black Holes (PBHs). PBHs represent hypothetical black holes produced by gravitational overdensities in the early Universe [14–16] and they lately sparkled the interest of the astroparticle community because of their particle production due to Hawking radiation [17]. Indeed, PBHs should be unstable and thermally emit particles depending on their mass [18, 19]. Within the conventional scenario, only PBHs with masses above 10^{15} g survive longer than the current age of the Universe, thereby remaining viable Dark Matter (DM) candidates. Nevertheless, existing observational constraints strongly limit the possibility that PBHs constitute the entirety of the DM abundance, confining this scenario primarily to the asteroid-mass window 10^{17} g $\lesssim M_{\text{PBH}} \lesssim 10^{22}$ g [20–23]. In contrast, lighter PBHs with $M_{\text{PBH}} \lesssim 10^{15}$ g, despite having evaporated by the present epoch, can still play an important phenomenological role, as their presence in the early Universe may have impacted several cosmological processes. For example, PBHs have been proposed to influence mechanisms responsible for generating the baryon asymmetry [24–38], act as sources of gravitational

waves [39–43], and contribute to DM production mechanisms [44–58].

In this framework, Refs. [59–61] have recently explored the back-reaction of particles on the quantum states of black holes, deducing that the evaporation could be quenched when a big fraction of the initial mass is lost by the black hole. This effect, usually referred to as *memory burden*, implies that light PBHs with masses $M \lesssim 10^{15}$ g could still be evaporating, leading to important phenomenological signatures [62–93]. Given that the typical energy of the emitted particles is set by the PBH temperature, which in turn depends inversely on its mass, sufficiently light PBHs can radiate extremely energetic particles. In particular, for $M_{\text{PBH}} \lesssim 10^4$ g, the characteristic emission energy reaches $\gtrsim 10^{18}$ eV. In this regime, UHECRs provide a unique and previously unexplored avenue to probe memory-burdened PBHs, opening a complementary window with respect to traditional gamma-ray and neutrino searches. Specifically, we exploit the UHECR flux and composition measurements [1, 94–97] as well as the upper limits on Ultra-High-Energy (UHE) neutrons [98] set by the Pierre Auger Observatory in order to constrain the abundance of PBHs in a range of energy not probed before.

The paper is organized as follows. In Sec. II we detail the Hawking evaporation of memory-burdened PBHs. In Sec. III we describe the computation of the UHECR flux from the galactic and extragalactic distributions of PBHs considered as a DM component. In Sec. IV we discuss the data samples and the statistical analysis used to derive the constraints on parameter space of memory-burdened PBH, which are then reported in Sec. V. Finally, in Sec. VI we draw our conclusions.

* antonio.ambrosone@gssi.it

† m.chianese@ssmeridionale.it

‡ carmelo.evoli@gssi.it

II. EVAPORATION OF MEMORY-BURDENED BLACK HOLES

Quantum field theory predicts that black holes are not perfectly stable objects but instead emit particles continuously. This phenomenon, known as Hawking evaporation, produces radiation that is nearly thermal, with a characteristic temperature set by the black hole mass:

$$T_{\text{H}} = \frac{1}{8\pi G M_{\text{PBH}}} \simeq 10^9 \left(\frac{10^4 \text{ g}}{M_{\text{PBH}}} \right) \text{ GeV}, \quad (1)$$

where G is Newton's constant and M_{PBH} denotes the PBH mass. This emission induces a gradual decrease of the PBH mass over time. This mass depletion is governed by

$$\frac{dM_{\text{PBH}}}{dt} = -\frac{\mathcal{G}g_{\text{SM}}}{30720\pi G^2 M_{\text{PBH}}^2}, \quad (2)$$

where $\mathcal{G} \simeq 3.8$ parametrizes the gray-body corrections arising from the scattering of particles in the curved spacetime surrounding the black hole [99]. The factor $g_{\text{SM}} \simeq 102.6$ counts the effective number of relativistic Standard Model degrees of freedom accessible at high Hawking temperatures [100]. Within the standard evaporation picture, this process proceeds uninterrupted until the PBH mass is entirely radiated away. Integrating the mass-loss equation (2) yields the total lifetime of a PBH:

$$\tau_{\text{PBH}} = \frac{10240\pi G^2 M_{\text{PBH}}^3}{\mathcal{G}g_{\text{SM}}} \simeq 4.4 \times 10^{17} \left(\frac{M_{\text{PBH}}}{10^{15} \text{ g}} \right)^3 \text{ s}. \quad (3)$$

Consequently, PBHs lighter than approximately 10^{15} g are expected to have completely evaporated by the present epoch.

In the memory-burden scenario, instead, the evaporation process separates into two distinct regimes. At early times, the PBH evolves as in the conventional Hawking picture, with its mass decreasing according to the standard evaporation law given by Eq. (2). This semiclassical regime persists until quantum information stored on the horizon becomes dynamically relevant. In the limit of an abrupt onset of the memory effects, this change of behavior takes place at

$$t_q = \tau_{\text{PBH}}(1 - q^3), \quad (4)$$

by which point the PBH retains only a fraction q of its original mass,

$$M_{\text{PBH}}^{\text{mb}} = qM_{\text{PBH}}. \quad (5)$$

Beyond t_q , the rate of mass loss is suppressed relative to the Hawking prediction as

$$\frac{dM_{\text{PBH}}^{\text{mb}}}{dt} = S(M_{\text{PBH}})^{-k} \frac{dM_{\text{PBH}}}{dt}, \quad (6)$$

where $k > 0$ controls the strength of the suppression which depends on the black hole's entropy defined by the

Bekenstein–Hawking formula $S(M_{\text{PBH}}) = 4\pi G M_{\text{PBH}}^2$. Integrating the modified evolution equation yields the PBH mass as a function of time during the memory-dominated regime:

$$M_{\text{PBH}}^{\text{mb}}(t) = M_{\text{PBH}}^{\text{mb}} \left[1 - \Gamma_{\text{PBH}}^{(k)}(t - t_q) \right]^{\frac{1}{3+2k}}, \quad (7)$$

where the effective decay rate is equal to

$$\Gamma_{\text{PBH}}^{(k)} = \frac{\mathcal{G}g_{\text{SM}}}{7680\pi} 2^k (3 + 2k) M_{\text{P}} \left(\frac{M_{\text{P}}}{M_{\text{PBH}}^{\text{mb}}} \right)^{3+2k}, \quad (8)$$

with $M_{\text{P}} = 1/\sqrt{8\pi G}$ denoting the reduced Planck mass.

The suppression of evaporation substantially prolongs the PBH lifetime. The total evaporation time is therefore dominated by the memory-burdened phase and can be approximated as

$$\tau_{\text{PBH}}^{(k)} = t_q + \left(\Gamma_{\text{PBH}}^{(k)} \right)^{-1} \simeq \left(\Gamma_{\text{PBH}}^{(k)} \right)^{-1}. \quad (9)$$

This extended lifetime may exceed the standard Hawking evaporation time by many orders of magnitude, opening the possibility that PBHs with much smaller initial masses survive until today. Such long-lived remnants could thus constitute a non-negligible component of the present-day DM abundance.

Throughout this work we adopt a reference value $q = 1/2$, motivated by the expectation that quantum memory effects become dynamically important once a black hole has radiated away roughly half of its initial mass. The exact numerical choice of q does not affect the qualitative behavior of the evaporation process, but instead determines how the derived bounds map onto the PBH mass at formation. Moreover, for the sake of simplicity, we model the onset of the memory-dominated regime as occurring instantaneously, treating the crossover from semiclassical evaporation to the suppressed phase as instantaneous. While this approximation captures the essential phenomenology relevant for our purposes, recent works [83, 84] indicate that a smooth or delayed transition may occur, thus modifying the PBH mass evolution over cosmological timescales. Importantly, the observational constraints considered in this study are mainly driven by present-day CR emission from the galactic halo. As a result, our bounds are largely insensitive to the detailed early-time behavior of the evaporation process. The limits presented here can therefore be straightforwardly reinterpreted within alternative frameworks featuring non-instantaneous suppression, provided the corresponding modification to the late-time evaporation rate is specified. A systematic treatment of such extended scenarios is left for future investigation.

III. THE COSMIC-RAY FLUX FROM PRIMORDIAL BLACK HOLES

We here detail the computation of the CR flux emitted by a population of memory-burdened PBHs, which

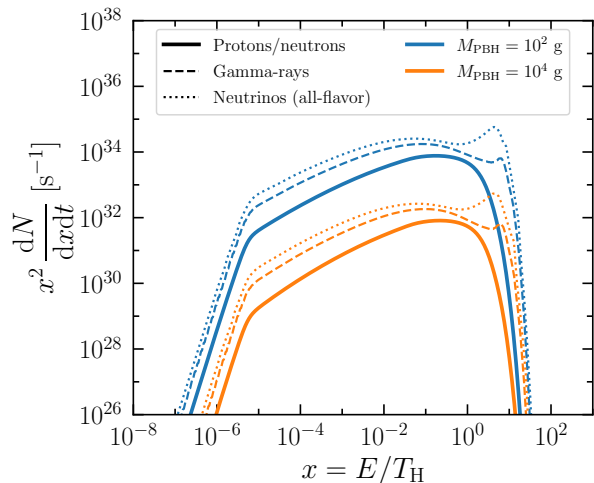


FIG. 1. Proton/neutron (solid lines), gamma-ray (dashed lines) and neutrino (dotted lines) energy spectra from PBH evaporation, shown as functions of $x = E/T_H$. The proton, neutron, and neutrino spectra include the sum of particle and antiparticle contributions. Results are displayed for two benchmark PBH masses: $M_{\text{PBH}} = 10^2$ g (blue curves) and $M_{\text{PBH}} = 10^4$ g (orange curves).

accounts for a fraction $f_{\text{PBH}} = \Omega_{\text{PBH}}/\Omega_{\text{DM}}$ of the total DM density of the Universe. We assume a monochromatic PBH mass spectrum within the range 10^{-1} g $\leq M_{\text{PBH}} \leq 10^7$ g.

In the presence of memory effects, the Hawking emission is globally attenuated according to Eq. (6). As a result, the primary emission rate of particles of species i from a non-rotating, neutral PBH of mass M_{PBH} is expected to be

$$\frac{d^2 N_i^{\text{mb}}}{dE dt} = S(M_{\text{PBH}})^{-k} \frac{d^2 N_i}{dE dt}, \quad (10)$$

where the quantity

$$\frac{d^2 N_i}{dE dt} = \frac{g_i}{2\pi} \frac{\mathcal{F}_i(E, M_{\text{PBH}})}{e^{E/T_H} - (-1)^{2s_i}}, \quad (11)$$

is the semi-classical emission rate with g_i and s_i denoting the internal degrees of freedom and the spin of the particles, respectively, and $\mathcal{F}_i(E, M_{\text{PBH}})$ being the graybody factor. The suppression factor of $S(M_{\text{PBH}})^{-k}$ affects the normalization of the spectrum without altering its characteristic energy scale: the maximum of the distribution continues to track the Hawking temperature, as in the standard semi-classical description. The primary emission from PBHs covers all elementary particles with masses below the Hawking temperature and, for light PBHs, it includes the entire Standard Model particle content.¹ Hadrons such as protons and neutrons

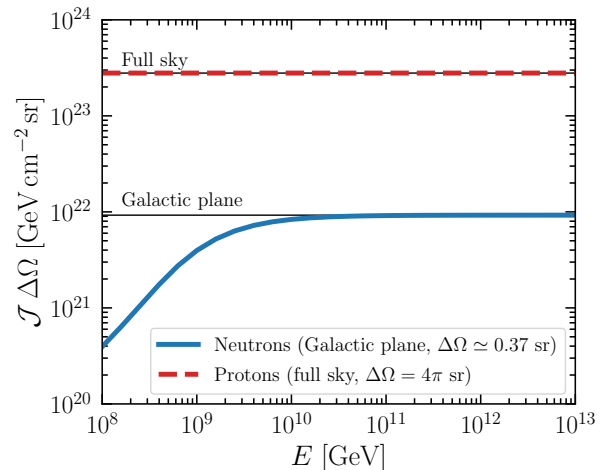


FIG. 2. The angle-integrated J-factor as a function of the energy for the neutrons from the galactic plane (blue line), defined as the region $0^\circ < l < 360^\circ$ and $-1.7^\circ < b < 1.7^\circ$ in galactic coordinates, and for the protons from the full sky (dashed red line).

are then produced by the evolution and hadronization of the primary particles. Hence, the secondary spectrum of protons and neutrons can be computed through the convolution of the primary spectra with the fragmentation functions [101].

In this analysis, we use the publicly-available codes `BlackHawk` [18, 19] and `HDMSpectra` [101] which provides tables for the primary emission spectra of PBHs and the fragmentation functions, respectively. The latter, however, only provides the fragmentation functions of the particle i into protons, $\mathcal{D}_{i \rightarrow p}$. We therefore compute the spectrum of neutrons by assuming an approximate isospin invariance between the up and down quarks, which implies $\mathcal{D}_{i \rightarrow p} \simeq \mathcal{D}_{i \rightarrow n}$ [102]. We also emphasize that the relative abundances of the emitted species from the PBH evaporation only scale with their internal degrees of freedom (see Eq. (11)). In Fig. 1, we show the proton and neutron spectra from the evaporation of a single PBH, compared to the corresponding gamma-ray and neutrino spectra, as functions of the dimensionless variable $x = E/T_H$, for representative benchmark values of M_{PBH} . In general, all spectra peak at energies $E \sim T_H$. Gamma-rays and neutrinos display fluxes larger by a factor of a few with respect to protons and neutrons, as they are produced both as primary particles and as secondary products of hadronization processes.

In order to evaluate the CR flux from the whole population of PBHs, we take into account both the galac-

spectra shown for species such as protons, neutrons, and neutrinos include the sum of particle and antiparticle contributions. The neutrino spectrum is computed following the appendix in Ref. [85] in order to avoid double counting of the primary emission.

¹ PBHs emit particles and antiparticles with equal probability. All

tic and extragalactic contributions. The angle-averaged galactic contribution from a region in the sky $\Delta\Omega$ can be calculated as

$$\frac{d^2\phi_{\text{CR}}^{\text{gal}}}{dE d\Omega} = \frac{f_{\text{PBH}}}{4\pi M_{\text{PBH}}^{\text{mb}}} \frac{d^2 N_{\text{CR}}^{\text{mb}}}{dE dt} \mathcal{J}(E, \Delta\Omega), \quad (12)$$

where the quantity

$$\mathcal{J}(E, \Omega) = \int_{\Delta\Omega} \frac{d\Omega}{\Delta\Omega} \int_0^{+\infty} ds \rho_{\text{PBH}}(r) e^{-s/L_{\text{CR}}(E)}, \quad (13)$$

is the J-factor which depends on the PBH density distribution within the Galaxy, $\rho_{\text{PBH}}(r)$, and takes into account the CR attenuation through the exponential factor. Following Refs. [62, 63], we consider the Navarro-Frank-White profile [103] for the PBH galactic distribution, namely

$$\rho_{\text{PBH}}(r) = \frac{\rho_s}{r/r_s (1 + r/r_s)^2}, \quad (14)$$

where $r_s = 25 \text{ kpc}$ and $\rho_s = 0.23 \text{ GeV cm}^{-3}$ [104], and $r = (s^2 + R_\odot^2 - 2sR_\odot \cos b \cos l)^{1/2}$ is the radial distance from the galactic center with $R_\odot \simeq 8.178 \text{ kpc}$ being the Sun distance from the galactic center [105]. In Eq. (12), the quantity L_{CR} represents the decay length for cosmic rays, which is infinity for protons being stable particles, while for neutrons it is $L_n(E) \simeq 8.5 (E/\text{EeV}) \text{ kpc}$ [98]. In the energy range relevant for this work, Galactic proton energy losses can be neglected because their interaction length is longer than typical galactic distances, in agreement with Ref. [7].

Figure 2 reports the angle-integrated J-factor as a function of energy for the neutrons propagating in the galactic plane ($0^\circ < l < 360^\circ$ and $-1.7^\circ < b < 1.7^\circ$) and for the protons emitted from the full galactic volume. Neutrons exhibit an energy-increasing J-factor because of their decay, reaching about 4% of the total galactic plane contribution at $E = 10^8 \text{ GeV}$. In comparison, the galactic plane accounts for $\sim 3.7\%$ of the total J-factor of the Galaxy. However, due to the different sky coverage $\Delta\Omega$, the angle-averaged J-factor of the galactic plane results to be slightly larger than that of the full sky, the latter being equal to $2.2 \times 10^{22} \text{ GeV cm}^{-2}$, in agreement with Refs. [62, 63]. This is crucial because the neutron and proton data samples provide the integrated and the differential fluxes, respectively, implying a similar constraining power.

We account for the extragalactic protons, by solving their Boltzmann equation with the generation energy technique as explained in Refs. [106, 107]

$$\frac{d^2\phi_p^{\text{egal}}}{dE d\Omega} = \frac{\Omega_{\text{DM}} \rho_{\text{cr}} f_{\text{PBH}}}{4\pi M_{\text{PBH}}^{\text{mb}}} \int_0^{z_{\text{max}}} \frac{dz}{H(z)} \times \left(\frac{1}{1+z} \frac{dE_g}{dE} \frac{d^2 N_p^{\text{mb}}}{dE dt} \Big|_{E=E_g(E,z)} \right), \quad (15)$$

where $H(z) = H_0 \sqrt{\Omega_m(1+z)^3 + \Omega_\Lambda}$, with $\Omega_m = 0.31$, $\Omega_\Lambda = 0.69$, $H_0 = 67.74 \text{ km s}^{-1} \text{ Mpc}^{-1}$ being the Λ CDM cosmological parameters reported by the Planck Collaboration and $\rho_{\text{cr}} = 4.8 \times 10^{-6} \text{ GeV cm}^{-3}$ being the critical density of the Universe [108]. The expression is usually referred to as *universal spectrum*, where $E_g(E, z)$ denotes exactly the *generation energy*, that is the energy that a proton must have at redshift z in order to be observed with energy E today ($z = 0$) [106].

This quantity consistently encodes all relevant energy-loss processes during propagation, including adiabatic losses from cosmic expansion and interactions with background photons, namely electron-positron pair and photopion productions. These interactions are computed considering only the Cosmic Microwave Background (CMB) radiation, since the impact of the Extragalactic Background Light (EBL) is negligible [107]. We implement pair-production and photopion losses following Ref. [109] and Ref. [110], respectively.

The upper integration limit z_{max} corresponds to the maximal source redshift, which is set to $z_{\text{max}} = 5$, though we have verified that the contribution from higher values is negligible. We further assume that f_{PBH} is constant over cosmological timescales, thus fixing it to the same value as for the galactic component.

We neglect the direct extragalactic neutron component at Earth, since neutrons emitted by PBHs decay over distances much shorter than cosmological ones. For instance, at 10^{21} eV the neutron decay length is only $\sim 8.5 \text{ Mpc}$. Nevertheless, since neutron beta decay produces protons, we account for this contribution in the instantaneous-decay approximation by assuming that the proton injection term in Eq. 15 is twice the direct proton injection from PBHs.

In Fig. 3, we compare the all-particle [1] and the proton [95, 96] fluxes measured by the Pierre Auger Observatory with the corresponding spectra predicted from PBHs in case of some benchmark scenarios. The values of f_{PBH} are fixed to the 95% CL upper limits derived from the proton analysis discussed in the next sections. The solid and dot-dashed lines correspond to the total (galactic and extragalactic) and the extragalactic proton fluxes, respectively. Furthermore, the dashed lines show the angle-averaged neutron fluxes emitted by the memory-burdened PBHs from the galactic plane. Interestingly, we find that its magnitude at high energies, where the neutron decays are negligible, is the same as that of the diffuse proton flux, despite the smaller J-factor as shown in Fig. 2.

IV. STATISTICAL ANALYSIS

A. Neutrons

The Pierre Auger Observatory has reported strong limits on the UHE neutrons from the galactic plane [98] (defined as the region with $0^\circ < l < 360^\circ$ and $-1.7^\circ < b <$

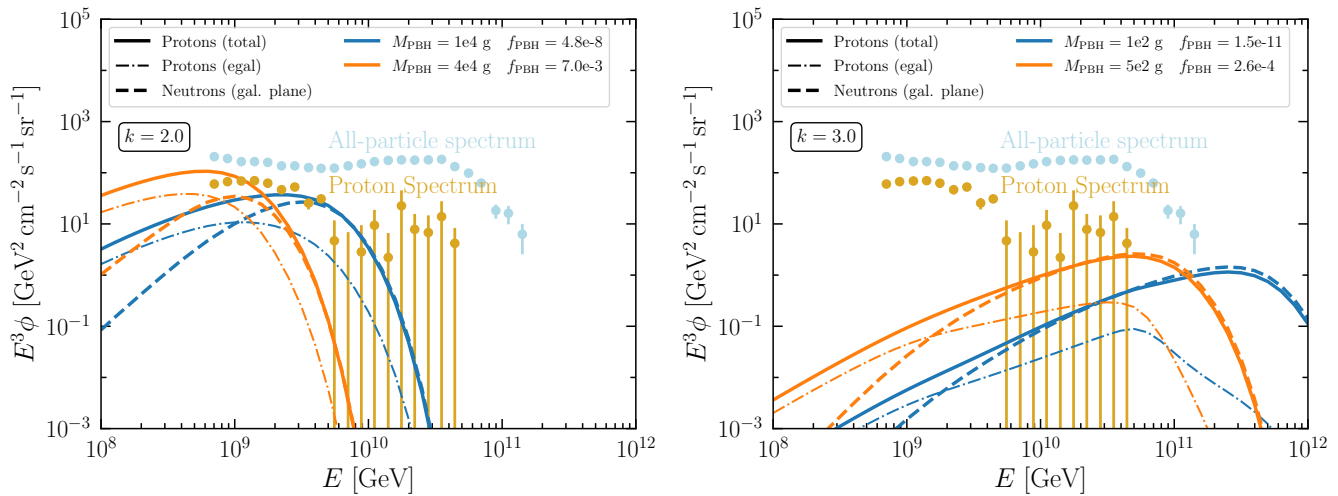


FIG. 3. The Auger All-particle [1] and proton [95, 96] spectra compared with the proton and neutron fluxes from PBHs fixing f_{PBH} at the 95% CL upper limit with protons. Left: memory-burden scenario with $k = 2$, for $M_{\text{PBH}} = 10^4$ g and $M_{\text{PBH}} = 4 \times 10^4$ g. Right: memory-burden scenario with $k = 3$, for $M_{\text{PBH}} = 100$ g and $M_{\text{PBH}} = 500$ g.

1.7°) with an integrated upper limit above 1 EeV of $\Phi_n = 0.077 \text{ km}^{-2} \text{ yr}^{-1}$ at 95% Confidence Level (CL). This indirectly constrains the neutrons emitted by memory-burdened PBHs according to the relation

$$\int_{1 \text{ EeV}}^{+\infty} dE \int_{\Delta\Omega} d\Omega \frac{d^2 \phi_n^{\text{gal}}}{dE d\Omega} \lesssim \Phi_n. \quad (16)$$

Here, the angular integral is evaluated over the galactic plane and the J-factor is given by the solid blue line in Fig. 2.

B. Protons

The measured UHECR flux extends from $\sim 7 \times 10^{17}$ eV up to $\sim 1.5 \times 10^{20}$ [1]. The mass composition suggests a light mass composition up to $\sim 10^{19}$ eV, with a trend of a heavier composition required to fit the data at higher energies [94–96]. In this work, to derive conservative proton-based constraints on PBHs, we adopt the proton spectrum ($\phi_p^{\text{Auger}}(E)$) inferred from the spectrum and composition measurements by Auger using the Sibyll 2.3d interaction model [96]. At energies above 5×10^{18} eV, where Auger reports only upper limits on the proton fraction, we impose that the proton spectrum does not exceed 10% of the all-particle spectrum ($\phi_{\text{all particle}}^{\text{Auger}}(E)$). This choice is consistent with the proton fraction inferred in Refs. [95, 96] and with the composition analysis [97]. Therefore, we define the chi-square difference as

$$\Delta\chi_p^2(f_{\text{PBH}}; \vec{\theta}_{\text{PBH}}) = \sum_i \begin{cases} \left(\frac{\mu_i - d_i}{\sigma_i}\right)^2 & \mu_i > d_i \\ 0 & \mu_i \leq d_i \end{cases}, \quad (17)$$

where the data d_i represent the inferred best-fit flux

$$d_i = \begin{cases} \phi_p^{\text{Auger}}(E_i) & E_i \leq 5 \times 10^{18} \text{ eV} \\ 0 & E_i > 5 \times 10^{18} \text{ eV} \end{cases}, \quad (18)$$

while σ_i are the uncertainties on the measured flux, which is conservatively set equal to $0.1 \phi_{\text{all particle}}^{\text{Auger}}(E)$ for $E \geq 5 \times 10^{18}$ eV.

$$\mu_i(f_{\text{PBH}}; \vec{\theta}_{\text{PBH}}) = \frac{d^2 \phi_p^{\text{gal}}}{dE d\Omega}(E_i) + \frac{d^2 \phi_p^{\text{egal}}}{dE d\Omega}(E_i), \quad (19)$$

which is a function of the PBH abundance f_{PBH} and $\vec{\theta}_{\text{PBH}} = (M_{\text{PBH}}, k)$. The angle-averaged galactic proton flux is computed over the entire solid angle, *i.e.* considering the J-factor given by the dashed red line in Fig. 2. Thus, for each combination of M_{PBH} and k , we determine the maximum allowed value for f_{PBH} following the Wilks' theorem under the assumption of a single degree of freedom [111].

V. RESULTS AND DISCUSSION

Fig. 4 reports the constraints on f_{PBH} in terms of M_{PBH} , for the memory-burden scenarios with $k = 2$ (left plot), $k = 3$ (center plot) and $k = 4$ (right plot). The results are also compared with the UHE gamma-rays and high-energy neutrino constraints obtained in Refs. [62] and [63], respectively. The hatched region shows the excluded region by the full evaporation of PBHs over cosmological timescales.

Interestingly, for $k = 2$ neutrons impose stronger constraints than protons, despite probing only a limited region of the Galaxy. By contrast, for $k = 3$ and $k = 4$ protons provide tighter constraints—by ~ 1 – 2 orders of

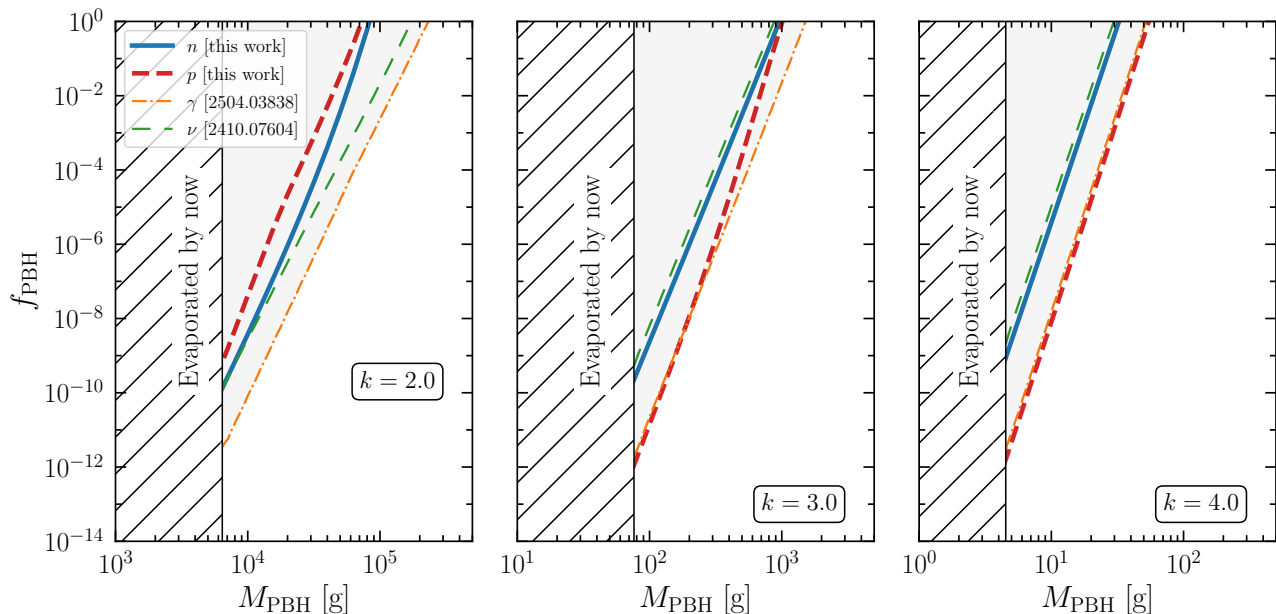


FIG. 4. Constraints at 95% CL on the fraction f_{PBH} as a function of the PBH mass at formation, in case of two scenarios for the memory-burden effect with $k = 2$ (left panel), $k = 3$ (middle panel) and $k = 4$ (right panel). The solid blue and dashed red lines represent the bounds derived in the present work from UHE neutrons and protons, respectively. The dot-dashed orange and long-dashed green lines correspond to the previous upper limits placed by UHE gamma-rays [62] and neutrinos [63], respectively (see also Refs. [64, 65, 73, 81, 85]). hatched region indicates PBHs that have fully evaporated over cosmological times.

magnitude—compared to neutrons. The origin of this difference lies in the energy dependence of the CR flux from PBHs: for $k = 2$ the emission peaks at 10^9 – 10^{10} GeV, where the measured proton flux is relatively high, leading to weaker proton constraints. Conversely, for $k \geq 3$ the PBH-induced flux is concentrated at higher energies, where the absence of observed protons severely restricts the allowed PBH emission. This is clearly shown in Fig. 3.

Interestingly, within this range of k , the bounds derived from protons are comparable in strength to those obtained from gamma rays in Ref. [62]. This result is non-trivial, given that gamma-ray fluxes are expected to be systematically larger than the proton ones, as discussed in Sec. III. The origin of this behavior lies in the dependence on k : for larger values of this parameter, the relevant PBH mass window shifts towards lower masses, corresponding to higher particle emission energies. As a consequence, differential flux limits derived from the non-observation of ultra-high-energy protons become increasingly competitive with the integral constraints obtained from gamma rays. Furthermore, as illustrated in the central panel of Fig. 4, proton limits degrade more rapidly with increasing initial PBH mass. This is expected, since larger PBH masses correspond to spectra that peak at lower energies, where the sensitivity of proton measurements becomes progressively weaker. In fact, smaller values of k would produce proton and neutron spectra peaking at lower energies, thereby leading to weaker CR

constraints. In this regime, other messengers such as gamma-rays and neutrinos provide significantly stronger limits [62, 63].

Fig. 5 shows the limit on M_{PBH} as a function of k , assuming $f_{\text{PBH}} = 1$. The hatched region reports the region where PBHs have fully evaporated over cosmological timescales, while the white portion above the constraints highlights the region where PBHs can fully constitute DM. The lines correspond to the obtained limits, demonstrating that for $k > 3$, CRs provide constraints slightly stronger than UHE gamma-rays, complementing their information regarding PBH constraints. For $k \lesssim 1.4$, instead, UHECRs are not sensitive to the emission from memory-burdened PBHs, which appears at lower energies (see Fig. 3).

VI. CONCLUSIONS

In this paper, we have explored the emission of UHE-CRs from memory-burdened PBHs. Indeed, the evaporation process induces a copious production of quarks which subsequently hadronize emitting protons and neutrons. Using the publicly-available `BlackHawk` and `HDMSPectra` codes, we have modeled the secondary proton and neutron emissions from a population of PBHs within the Milky Way, evaluating constraints on the PBH parameter space using limits imposed by the non-observations of neutrons and protons at the highest energies by the

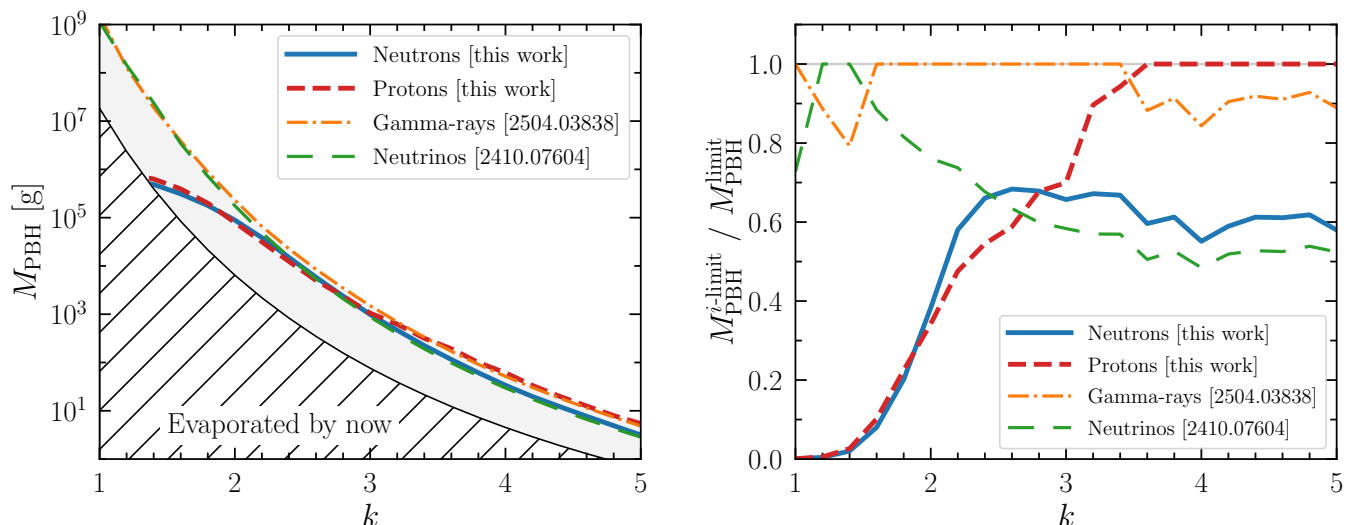


FIG. 5. Constraints on memory-burdened PBHs as viable DM candidates. Left: the different lines refer to limits placed at 95% CL in the k - M_{PBH} plane with $f_{\text{PBH}} = 1$ according to UHE protons (solid blue line), UHE neutrons (dashed red line), UHE gamma-rays (dot-dashed orange line) [62] and neutrinos (long-dashed green line) [63] (see also Refs. [64, 65, 73, 81, 85]). The white area represents the parameter space where memory-burdened PBHs can account for the total DM component of the Universe ($f_{\text{PBH}} = 1$), whereas the hatched region indicates PBHs that have fully evaporated over cosmological times. Right: ratio of the limits on M_{PBH} placed by the different data samples over the global bound in order to highlight the most constraining measurement.

Pierre Auger Observatory.

Despite implementing conservative statistical analyses, we have demonstrated that constraints with protons, for $k \gtrsim 3$ and $M_{\text{PBH}} \lesssim 500$ g, are as tight as than previous ones obtained with UHE gamma-rays, despite those are not only emitted as secondary particles during hadronization but also as primary ones.

By contrast, limits obtained from neutrons are generally weaker than those derived from gamma rays, as they similarly rely on integral flux limits and associated with an overall lower flux. Nonetheless, neutron bounds remain competitive, reaching sensitivities comparable to those obtained with high-energy neutrinos [63]. Future analyses could significantly improve these constraints by exploiting data by AugerPrime [112]—the upgrade of the Pierre Auger Experiment— as well as by implementing dedicated spatial-template analyses, potentially leading to much tighter bounds.

ACKNOWLEDGEMENTS

AA and CE gratefully acknowledge the PAO Collaboration for helpful discussions that contributed to

this work. The authors also acknowledge Daniele Gaggero for fruitful discussions throughout several stages of the manuscript. AA acknowledges the support of the project “NUSES - A pathfinder for studying astrophysical neutrinos and electromagnetic signals of seismic origin from space” (Cod. id. Ugov: NUSES; CUP: D12F19000040003). The work of CE has been partially funded by the European Union – Next Generation EU, through PRIN-MUR 2022TJW4EJ and by the European Union – NextGenerationEU under the MUR National Innovation Ecosystem grant ECS00000041 – VITALITY/ASTRA – CUP D13C21000430001. AA, MC and CE acknowledge the support by the research project TAsP (Theoretical Astroparticle Physics) funded by the Istituto Nazionale di Fisica Nucleare (INFN).

[1] P. Abreu *et al.* (Pierre Auger Collaboration), The energy spectrum of cosmic rays beyond the turn-down around 10^{17} eV as measured with the surface detector of the Pierre Auger Observatory, *Eur. Phys. J. C* **81**,

966 (2021), arXiv:2109.13400 [astro-ph.HE].

[2] T. Abu-Zayyad *et al.*, The Cosmic-Ray Energy Spectrum Observed with the Surface Detector of the Telescope Array Experiment, *ApJ* **768**, L1 (2013),

- arXiv:1205.5067 [astro-ph.HE].
- [3] R. Aloisio, A. Ambrosone, and C. Evoli, Constraining Super-Heavy Dark Matter with the KM3-230213A Neutrino Event, arXiv (2025), arXiv:2508.08779 [astro-ph.HE].
 - [4] M. Chianese, D. F. G. Fiorillo, R. Hajjar, G. Miele, and N. Saviano, Constraints on heavy decaying dark matter with current gamma-ray measurements, *JCAP* **11**, 035, arXiv:2108.01678 [hep-ph].
 - [5] P. Abreu *et al.* (Pierre Auger Collaboration), Cosmological implications of photon-flux upper limits at ultrahigh energies in scenarios of Planckian-interacting massive particles for dark matter, *Phys. Rev. D* **107**, 042002 (2023), arXiv:2208.02353 [astro-ph.HE].
 - [6] P. Abreu *et al.* (Pierre Auger Collaboration), Limits to Gauge Coupling in the Dark Sector Set by the Nonobservation of Instanton-Induced Decay of Super-Heavy Dark Matter in the Pierre Auger Observatory Data, *Phys. Rev. Lett.* **130**, 061001 (2023), arXiv:2203.08854 [astro-ph.HE].
 - [7] S. Das, K. Murase, and T. Fujii, Revisiting ultrahigh-energy constraints on decaying superheavy dark matter, *Phys. Rev. D* **107**, 103013 (2023), arXiv:2302.02993 [astro-ph.HE].
 - [8] C. Bérat, C. Bleve, O. Deligny, F. Montanet, P. Savina, and Z. Torrès, Diffuse Flux of Ultra-high-energy Photons from Cosmic-Ray Interactions in the Disk of the Galaxy and Implications for the Search for Decaying Super-heavy Dark Matter, *Astrophys. J.* **929**, 55 (2022), arXiv:2203.08751 [astro-ph.HE].
 - [9] R. Aloisio and F. Tortorici, Super Heavy Dark Matter and UHECR Anisotropy at Low Energy, *Astropart. Phys.* **29**, 307 (2008), arXiv:0706.3196 [astro-ph].
 - [10] A. A. Halim *et al.* (Pierre Auger Collaboration), Search for a diffuse flux of photons with energies above tens of PeV at the Pierre Auger Observatory, *JCAP* **05**, 061, arXiv:2502.02381 [astro-ph.HE].
 - [11] A. Abdul Halim *et al.* (Pierre Auger Collaboration), Constraints on metastable superheavy dark matter coupled to sterile neutrinos with the Pierre Auger Observatory, *Phys. Rev. D* **109**, L081101 (2024), arXiv:2311.14541 [hep-ph].
 - [12] P. Abreu *et al.* (Pierre Auger Collaboration), Testing effects of Lorentz invariance violation in the propagation of astroparticles with the Pierre Auger Observatory, *JCAP* **01** (01), 023, arXiv:2112.06773 [astro-ph.HE].
 - [13] M. Chianese, N. Saviano, S. Cesare, V. M. Grieco, V. Nasti, F. Spinnato, and A. Tiano, Probing super-heavy dark matter with ultra-high-energy gamma rays, (2026), arXiv:2601.11703 [hep-ph].
 - [14] Y. B. Zel'dovich and I. D. Novikov, The Hypothesis of Cores Retarded during Expansion and the Hot Cosmological Model, *Sov. Astron.* **10**, 602 (1967).
 - [15] S. Hawking, Gravitationally collapsed objects of very low mass, *Mon. Not. Roy. Astron. Soc.* **152**, 75 (1971).
 - [16] B. J. Carr and S. W. Hawking, Black holes in the early Universe, *Mon. Not. Roy. Astron. Soc.* **168**, 399 (1974).
 - [17] S. W. Hawking, Black hole explosions, *Nature* **248**, 30 (1974).
 - [18] A. Arbey and J. Auffinger, BlackHawk: A public code for calculating the Hawking evaporation spectra of any black hole distribution, *Eur. Phys. J. C* **79**, 693 (2019), arXiv:1905.04268 [gr-qc].
 - [19] A. Arbey and J. Auffinger, Physics Beyond the Standard Model with BlackHawk v2.0, *Eur. Phys. J. C* **81**, 910 (2021), arXiv:2108.02737 [gr-qc].
 - [20] B. Carr, F. Kuhnel, and M. Sandstad, Primordial Black Holes as Dark Matter, *Phys. Rev. D* **94**, 083504 (2016), arXiv:1607.06077 [astro-ph.CO].
 - [21] A. M. Green and B. J. Kavanagh, Primordial Black Holes as a dark matter candidate, *J. Phys. G* **48**, 043001 (2021), arXiv:2007.10722 [astro-ph.CO].
 - [22] B. Carr, K. Kohri, Y. Sendouda, and J. Yokoyama, Constraints on primordial black holes, *Rept. Prog. Phys.* **84**, 116902 (2021), arXiv:2002.12778 [astro-ph.CO].
 - [23] B. Carr and F. Kuhnel, Primordial black holes as dark matter candidates, *SciPost Phys. Lect. Notes* **48**, 1 (2022), arXiv:2110.02821 [astro-ph.CO].
 - [24] T. Fujita, M. Kawasaki, K. Harigaya, and R. Matsuda, Baryon asymmetry, dark matter, and density perturbation from primordial black holes, *Phys. Rev. D* **89**, 103501 (2014), arXiv:1401.1909 [astro-ph.CO].
 - [25] Y. Hamada and S. Iso, Baryon asymmetry from primordial black holes, *PTEP* **2017**, 033B02 (2017), arXiv:1610.02586 [hep-ph].
 - [26] L. Morrison, S. Profumo, and Y. Yu, Melanogenesis: Dark Matter of (almost) any Mass and Baryonic Matter from the Evaporation of Primordial Black Holes weighing a Ton (or less), *JCAP* **05**, 005, arXiv:1812.10606 [astro-ph.CO].
 - [27] S.-L. Chen, A. Dutta Banik, and Z.-K. Liu, Leptogenesis in fast expanding Universe, *JCAP* **03**, 009, arXiv:1912.07185 [hep-ph].
 - [28] Y. F. Perez-Gonzalez and J. Turner, Assessing the tension between a black hole dominated early universe and leptogenesis, *Phys. Rev. D* **104**, 103021 (2021), arXiv:2010.03565 [hep-ph].
 - [29] S. Datta, A. Ghosal, and R. Samanta, Baryogenesis from ultralight primordial black holes and strong gravitational waves from cosmic strings, *JCAP* **08**, 021, arXiv:2012.14981 [hep-ph].
 - [30] D. Hooper and G. Krnjaic, GUT Baryogenesis With Primordial Black Holes, *Phys. Rev. D* **103**, 043504 (2021), arXiv:2010.01134 [hep-ph].
 - [31] S. Jyoti Das, D. Mahanta, and D. Borah, Low scale leptogenesis and dark matter in the presence of primordial black holes, *JCAP* **11**, 019, arXiv:2104.14496 [hep-ph].
 - [32] V. De Luca, G. Franciolini, A. Kehagias, and A. Riotto, Standard model baryon number violation seeded by black holes, *Phys. Lett. B* **819**, 136454 (2021), arXiv:2102.07408 [astro-ph.CO].
 - [33] N. Bernal, C. S. Fong, Y. F. Perez-Gonzalez, and J. Turner, Rescuing high-scale leptogenesis using primordial black holes, *Phys. Rev. D* **106**, 035019 (2022), arXiv:2203.08823 [hep-ph].
 - [34] R. Calabrese, M. Chianese, J. Gunn, G. Miele, S. Morisi, and N. Saviano, Limits on light primordial black holes from high-scale leptogenesis, *Phys. Rev. D* **107**, 123537 (2023), arXiv:2305.13369 [hep-ph].
 - [35] R. Calabrese, M. Chianese, J. Gunn, G. Miele, S. Morisi, and N. Saviano, Impact of primordial black holes on heavy neutral leptons searches in the framework of resonant leptogenesis, *Phys. Rev. D* **109**, 103001 (2024), arXiv:2311.13276 [hep-ph].
 - [36] K. Schmitz and X.-J. Xu, Wash-in leptogenesis after the evaporation of primordial black holes, *Phys. Lett. B* **849**, 138473 (2024), arXiv:2311.01089 [hep-ph].

- [37] B. Barman, S. Jyoti Das, M. R. Haque, and Y. Mambrini, Leptogenesis, primordial gravitational waves, and PBH-induced reheating, *Phys. Rev. D* **110**, 043528 (2024), [arXiv:2403.05626 \[hep-ph\]](#).
- [38] J. Gunn, L. Heurtier, Y. F. Perez-Gonzalez, and J. Turner, Primordial black hole hot spots and out-of-equilibrium dynamics, *JCAP* **02**, 040, [arXiv:2409.02173 \[hep-ph\]](#).
- [39] T. Papanikolaou, V. Vennin, and D. Langlois, Gravitational waves from a universe filled with primordial black holes, *JCAP* **03**, 053, [arXiv:2010.11573 \[astro-ph.CO\]](#).
- [40] G. Domènech, C. Lin, and M. Sasaki, Gravitational wave constraints on the primordial black hole dominated early universe, *JCAP* **04**, 062, [Erratum: *JCAP* **11**, E01 (2021)], [arXiv:2012.08151 \[gr-qc\]](#).
- [41] T. Papanikolaou, Gravitational waves induced from primordial black hole fluctuations: the effect of an extended mass function, *JCAP* **10**, 089, [arXiv:2207.11041 \[astro-ph.CO\]](#).
- [42] A. Ireland, S. Profumo, and J. Scharnhorst, Primordial gravitational waves from black hole evaporation in standard and nonstandard cosmologies, *Phys. Rev. D* **107**, 104021 (2023), [arXiv:2302.10188 \[gr-qc\]](#).
- [43] G. Domènech and J. Tränkle, From formation to evaporation: Induced gravitational wave probes of the primordial black hole reheating scenario, *Phys. Rev. D* **111**, 063528 (2025), [arXiv:2409.12125 \[gr-qc\]](#).
- [44] N. Bernal and Ó. Zapata, Self-interacting Dark Matter from Primordial Black Holes, *JCAP* **03**, 007, [arXiv:2010.09725 \[hep-ph\]](#).
- [45] P. Gondolo, P. Sandick, and B. Shams Es Haghi, Effects of primordial black holes on dark matter models, *Phys. Rev. D* **102**, 095018 (2020), [arXiv:2009.02424 \[hep-ph\]](#).
- [46] N. Bernal and Ó. Zapata, Gravitational dark matter production: primordial black holes and UV freeze-in, *Phys. Lett. B* **815**, 136129 (2021), [arXiv:2011.02510 \[hep-ph\]](#).
- [47] N. Bernal and Ó. Zapata, Dark Matter in the Time of Primordial Black Holes, *JCAP* **03**, 015, [arXiv:2011.12306 \[astro-ph.CO\]](#).
- [48] A. Cheek, L. Heurtier, Y. F. Perez-Gonzalez, and J. Turner, Primordial black hole evaporation and dark matter production. I. Solely Hawking radiation, *Phys. Rev. D* **105**, 015022 (2022), [arXiv:2107.00013 \[hep-ph\]](#).
- [49] A. Cheek, L. Heurtier, Y. F. Perez-Gonzalez, and J. Turner, Primordial black hole evaporation and dark matter production. II. Interplay with the freeze-in or freeze-out mechanism, *Phys. Rev. D* **105**, 015023 (2022), [arXiv:2107.00016 \[hep-ph\]](#).
- [50] R. Samanta and F. R. Urban, Testing super heavy dark matter from primordial black holes with gravitational waves, *JCAP* **06** (06), 017, [arXiv:2112.04836 \[hep-ph\]](#).
- [51] N. Bernal, F. Hajkarim, and Y. Xu, Axion Dark Matter in the Time of Primordial Black Holes, *Phys. Rev. D* **104**, 075007 (2021), [arXiv:2107.13575 \[hep-ph\]](#).
- [52] N. Bernal, Y. F. Perez-Gonzalez, Y. Xu, and Ó. Zapata, ALP dark matter in a primordial black hole dominated universe, *Phys. Rev. D* **104**, 123536 (2021), [arXiv:2110.04312 \[hep-ph\]](#).
- [53] P. Sandick, B. S. Es Haghi, and K. Sinha, Asymmetric reheating by primordial black holes, *Phys. Rev. D* **104**, 083523 (2021), [arXiv:2108.08329 \[astro-ph.CO\]](#).
- [54] N. Bernal, Y. F. Perez-Gonzalez, and Y. Xu, Super-radiant production of heavy dark matter from primordial black holes, *Phys. Rev. D* **106**, 015020 (2022), [arXiv:2205.11522 \[hep-ph\]](#).
- [55] A. Cheek, L. Heurtier, Y. F. Perez-Gonzalez, and J. Turner, Evaporation of primordial black holes in the early Universe: Mass and spin distributions, *Phys. Rev. D* **108**, 015005 (2023), [arXiv:2212.03878 \[hep-ph\]](#).
- [56] T. C. Gehrman, B. Shams Es Haghi, K. Sinha, and T. Xu, Recycled dark matter, *JCAP* **03**, 044, [arXiv:2310.08526 \[hep-ph\]](#).
- [57] E. Bertuzzo, Y. F. Perez-Gonzalez, G. M. Salla, and R. Z. Funchal, Gravitationally produced dark matter and primordial black holes, *JCAP* **09**, 059, [arXiv:2405.17611 \[hep-ph\]](#).
- [58] G. Franciolini and D. Racco, Isocurvature Constraints on Dark Matter from Evaporated Primordial Black Holes, (2026), [arXiv:2603.02322 \[astro-ph.CO\]](#).
- [59] G. Dvali, A Microscopic Model of Holography: Survival by the Burden of Memory, *arXiv* (2018), [arXiv:1810.02336 \[hep-th\]](#).
- [60] G. Dvali, L. Eisemann, M. Michel, and S. Zell, Black hole metamorphosis and stabilization by memory burden, *Phys. Rev. D* **102**, 103523 (2020), [arXiv:2006.00011 \[hep-th\]](#).
- [61] G. Dvali, J. S. Valbuena-Bermúdez, and M. Zantedeschi, Memory burden effect in black holes and solitons: Implications for PBH, *Phys. Rev. D* **110**, 056029 (2024), [arXiv:2405.13117 \[hep-th\]](#).
- [62] M. Chianese, High-energy gamma-ray emission from memory-burdened primordial black holes, *Phys. Rev. D* **112**, 023043 (2025), [arXiv:2504.03838 \[astro-ph.HE\]](#).
- [63] M. Chianese, A. Boccia, F. Iocco, G. Miele, and N. Saviano, Light burden of memory: Constraining primordial black holes with high-energy neutrinos, *Phys. Rev. D* **111**, 063036 (2025), [arXiv:2410.07604 \[astro-ph.HE\]](#).
- [64] A. Alexandre, G. Dvali, and E. Koutsangelas, New mass window for primordial black holes as dark matter from the memory burden effect, *Phys. Rev. D* **110**, 036004 (2024), [arXiv:2402.14069 \[hep-ph\]](#).
- [65] V. Thoss, A. Burkert, and K. Kohri, Breakdown of hawking evaporation opens new mass window for primordial black holes as dark matter candidate, *Mon. Not. Roy. Astron. Soc.* **532**, 451 (2024), [arXiv:2402.17823 \[astro-ph.CO\]](#).
- [66] M. R. Haque, S. Maity, D. Maity, and Y. Mambrini, Quantum effects on the evaporation of PBHs: contributions to dark matter, *JCAP* **07**, 002, [arXiv:2404.16815 \[hep-ph\]](#).
- [67] S. Balaji, G. Domènech, G. Franciolini, A. Ganz, and J. Tränkle, Probing modified Hawking evaporation with gravitational waves from the primordial black hole dominated universe, *JCAP* **11**, 026, [arXiv:2403.14309 \[gr-qc\]](#).
- [68] B. Barman, M. R. Haque, and Ó. Zapata, Gravitational wave signatures of cogenesis from a burdened PBH, *JCAP* **09**, 020, [arXiv:2405.15858 \[astro-ph.CO\]](#).
- [69] N. Bhaumik, M. R. Haque, R. K. Jain, and M. Lewicki, Memory burden effect mimics reheating signatures on SGWB from ultra-low mass PBH domination, *JHEP* **10**, 142, [arXiv:2409.04436 \[astro-ph.CO\]](#).
- [70] B. Barman, K. Loho, and Ó. Zapata, Constraining burdened PBHs with gravitational waves, *JCAP* **10**, 065,

- arXiv:2409.05953 [gr-qc].
- [71] K. Kohri, T. Terada, and T. T. Yanagida, Induced gravitational waves probing primordial black hole dark matter with the memory burden effect, *Phys. Rev. D* **111**, 063543 (2025), arXiv:2409.06365 [astro-ph.CO].
- [72] Y. Jiang, C. Yuan, C.-Z. Li, and Q.-G. Huang, Constraints on the primordial black hole abundance through scalar-induced gravitational waves from Advanced LIGO and Virgo's first three observing runs, *JCAP* **12**, 016, arXiv:2409.07976 [astro-ph.CO].
- [73] M. Zantedeschi and L. Visinelli, Ultralight black holes as sources of high-energy particles, *Phys. Dark Univ.* **49**, 102034 (2025), arXiv:2410.07037 [astro-ph.HE].
- [74] W. Barker, B. Gladwyn, and S. Zell, Inflationary and gravitational wave signatures of small primordial black holes as dark matter, *Phys. Rev. D* **111**, 123033 (2025), arXiv:2410.11948 [astro-ph.CO].
- [75] D. Borah and N. Das, Successful co-genesis of baryon and dark matter from memory-burdened PBH, *JCAP* **02**, 031, arXiv:2410.16403 [hep-ph].
- [76] N. P. D. Loc, Gravitational waves from burdened primordial black holes dark matter, *Phys. Rev. D* **111**, 023509 (2025), arXiv:2410.17544 [gr-qc].
- [77] U. Basumatary, N. Raj, and A. Ray, Beyond Hawking evaporation of black holes formed by dark matter in compact stars, *Phys. Rev. D* **111**, L041306 (2025), arXiv:2410.22702 [hep-ph].
- [78] P. Athron, M. Chianese, S. Datta, R. Samanta, and N. Saviano, Impact of memory-burdened black holes on primordial gravitational waves in light of Pulsar Timing Array, *JCAP* **05**, 005, arXiv:2411.19286 [astro-ph.CO].
- [79] D. Bandyopadhyay, D. Borah, and N. Das, Axion misalignment with memory-burdened PBH, *JCAP* **04**, 039, arXiv:2501.04076 [hep-ph].
- [80] R. Calabrese, M. Chianese, and N. Saviano, Impact of memory-burdened primordial black holes on high-scale leptogenesis, *Phys. Rev. D* **111**, 083008 (2025), arXiv:2501.06298 [hep-ph].
- [81] A. Boccia and F. Iocco, Could the KM3-230213A event be caused by an evaporating primordial black hole?, *Phys. Rev. D* **112**, 063045 (2025), arXiv:2502.19245 [astro-ph.HE].
- [82] T.-C. Liu, B.-Y. Zhu, Y.-F. Liang, X.-S. Hu, and E.-W. Liang, Constraining the parameters of heavy dark matter and memory-burdened primordial black holes with DAMPE electron measurements, *JHEAp* **47**, 100375 (2025), arXiv:2503.13192 [astro-ph.HE].
- [83] G. Dvali, M. Zantedeschi, and S. Zell, Transitioning to Memory Burden: Detectable Small Primordial Black Holes as Dark Matter, arXiv (2025), arXiv:2503.21740 [hep-ph].
- [84] G. Montefalcone, D. Hooper, K. Freese, C. Kelso, F. Kuhnel, and P. Sandick, Does Memory Burden Open a New Mass Window for Primordial Black Holes as Dark Matter?, arXiv (2025), arXiv:2503.21005 [astro-ph.CO].
- [85] A. Donarini, G. Marino, P. Panci, and M. Zantedeschi, The fast, the slow and the merging: probes of evaporating memory burdened PBHs, *JCAP* **11**, 006, arXiv:2506.13861 [hep-ph].
- [86] N. Levy and L. Heurtier, Effect of the Memory Burden on Primordial Black Hole Hot Spots, arXiv (2025), arXiv:2511.17329 [astro-ph.CO].
- [87] P.-Y. Tseng and Y.-M. Yeh, Constraining memory-burdened primordial black holes with graviton-photon conversion and binary mergers, arXiv (2025), arXiv:2511.01848 [hep-ph].
- [88] A. Chaudhuri, K. Kohri, and V. Thoss, New bounds on memory burdened primordial black holes from Big Bang nucleosynthesis, *JCAP* **11**, 057, arXiv:2506.20717 [astro-ph.CO].
- [89] T. Kitabayashi and A. Takeshita, WIMP/FIMP dark matter and primordial black holes with memory burden effect, arXiv (2025), arXiv:2506.20071 [hep-ph].
- [90] X.-h. Tan and Y.-f. Zhou, Probing Memory-Burdened Primordial Black Holes with Galactic Sources observed by LHAASO, arXiv (2025), arXiv:2505.19857 [astro-ph.CO].
- [91] A. Chaudhuri, K. Pal, and R. Mohanta, Neutrino Fluence influenced by Memory Burdened Primordial Black Holes, arXiv (2025), arXiv:2505.09153 [hep-ph].
- [92] S. Maity, Relativistic accretion and burdened primordial black holes, arXiv (2025), arXiv:2507.02821 [astro-ph.CO].
- [93] M. Merchand, Exploring Ultra-Slow-Roll Inflation in Composite Pseudo-Nambu-Goldstone Boson Models: Implications for Primordial Black Holes and Gravitational Waves, arXiv (2025), arXiv:2510.15460 [astro-ph.CO].
- [94] A. Aab *et al.* (The Pierre Auger Collaboration), Measurement of the cosmic-ray energy spectrum above 2.5×10^{18} eV using the pierre auger observatory, *Phys. Rev. D* **102**, 062005 (2020).
- [95] A. Abdul Halim *et al.*, Depth of Maximum of Air-Shower Profiles above $10^{17.8}$ eV Measured with the Fluorescence Detector of the Pierre Auger Observatory and Mass Composition Implications, *PoS ICRC2023*, 319 (2023).
- [96] A. Abdul Halim *et al.*, Studies of the mass composition of cosmic rays and proton-proton interaction cross-sections at ultra-high energies with the Pierre Auger Observatory, *PoS ICRC2023*, 438 (2023).
- [97] A. Abdul Halim *et al.* (Pierre Auger Collaboration), Inference of the Mass Composition of Cosmic Rays with Energies from 1018.5 to 1020 eV Using the Pierre Auger Observatory and Deep Learning, *Phys. Rev. Lett.* **134**, 021001 (2025), arXiv:2406.06315 [astro-ph.HE].
- [98] A. Aab *et al.* (Pierre Auger Collaboration), A Targeted Search for Point Sources of EeV Neutrons, *Astrophys. J. Lett.* **789**, L34 (2014), arXiv:1406.4038 [astro-ph.HE].
- [99] D. N. Page and S. W. Hawking, Gamma rays from primordial black holes, *Astrophys. J.* **206**, 1 (1976).
- [100] K. Mazde and L. Visinelli, The interplay between the dark matter axion and primordial black holes, *JCAP* **01**, 021, arXiv:2209.14307 [astro-ph.CO].
- [101] C. W. Bauer, N. L. Rodd, and B. R. Webber, Dark matter spectra from the electroweak to the Planck scale, *JHEP* **06**, 121, arXiv:2007.15001 [hep-ph].
- [102] S. Navas *et al.* (Particle Data Group), Review of particle physics, *Phys. Rev. D* **110**, 030001 (2024).
- [103] J. F. Navarro, C. S. Frenk, and S. D. M. White, The Structure of cold dark matter halos, *Astrophys. J.* **462**, 563 (1996), arXiv:astro-ph/9508025.
- [104] M. Benito, F. Iocco, and A. Cuoco, Uncertainties in the Galactic Dark Matter distribution: An update, *Phys. Dark Univ.* **32**, 100826 (2021), arXiv:2009.13523 [astro-ph.GA].

- [105] R. Abuter *et al.* (Gravity), A geometric distance measurement to the Galactic center black hole with 0.3% uncertainty, *Astron. Astrophys.* **625**, [10.1051/0004-6361/201935656](https://doi.org/10.1051/0004-6361/201935656) (2019), [arXiv:1904.05721](https://arxiv.org/abs/1904.05721) [[astro-ph.GA](#)].
- [106] A. Cermenati, A. Ambrosone, R. Aloisio, D. Boncioli, and C. Evoli, Scrutinizing the cosmogenic origin of the KM3-230213A event: A Multimessenger Perspective, *arXiv* (2025), [arXiv:2507.11993](https://arxiv.org/abs/2507.11993) [[astro-ph.HE](#)].
- [107] V. Berezhinsky, A. Z. Gazizov, and S. I. Grigorieva, On astrophysical solution to ultrahigh-energy cosmic rays, *Phys. Rev. D* **74**, 043005 (2006), [arXiv:hep-ph/0204357](https://arxiv.org/abs/hep-ph/0204357).
- [108] N. Aghanim *et al.* (Planck), Planck 2018 results. VI. Cosmological parameters, *Astron. Astrophys.* **641**, A6 (2020), [Erratum: *Astron. Astrophys.* 652, C4 (2021)], [arXiv:1807.06209](https://arxiv.org/abs/1807.06209) [[astro-ph.CO](#)].
- [109] G. R. Blumenthal, Energy loss of high-energy cosmic rays in pair-producing collisions with ambient photons, *Phys. Rev. D* **1**, 1596 (1970).
- [110] S. R. Kelner and F. A. Aharonian, Energy spectra of gamma-rays, electrons and neutrinos produced at interactions of relativistic protons with low energy radiation, *Phys. Rev. D* **78**, 034013 (2008), [Erratum: *Phys. Rev. D* 82, 099901 (2010)], [arXiv:0803.0688](https://arxiv.org/abs/0803.0688) [[astro-ph](#)].
- [111] G. Cowan, K. Cranmer, E. Gross, and O. Vitells, Asymptotic formulae for likelihood-based tests of new physics, *Eur. Phys. J. C* **71**, 1554 (2011), [Erratum: *Eur. Phys. J. C* 73, 2501 (2013)], [arXiv:1007.1727](https://arxiv.org/abs/1007.1727) [[physics.data-an](#)].
- [112] A. Castellina (Pierre Auger Collaboration), Auger-Prime: the Pierre Auger Observatory Upgrade, *EPJ Web Conf.* **210**, 06002 (2019), [arXiv:1905.04472](https://arxiv.org/abs/1905.04472) [[astro-ph.HE](#)].